JOURNAL OF MAGNETIC RESONANCE IMAGING 31:168–176 (2010)

Original Research

Scan-Rescan Reproducibility of Carotid Atherosclerotic Plaque Morphology and Tissue Composition Measurements Using Multicontrast MRI at 3T

Feiyu Li, MD,[1,2] Vasily L. Yarnykh, PhD,[1] Thomas S. Hatsukami, MD,[3] Baocheng Chu, MD, PhD,[1] Niranjan Balu, PhD,[1] Jinnan Wang, PhD,[4] Hunter R. Underhill, MD,[1] Xihai Zhao, MD,[1] Robin Smith, BS,[1] and Chun Yuan, PhD[1]*

Purpose: To evaluate interscan reproducibility of both vessel morphology and tissue composition measurements of carotid atherosclerosis using a fast, optimized, 3T multicontrast protocol.

Materials and Methods: A total of 20 patients with carotid stenosis >15% identified by duplex ultrasound were recruited for two independent 3T MRI (Philips) scans within one month. A multicontrast protocol including five MR sequences was applied: TOF, T1-/T2-/PD-weighted and magnetization-prepared rapid acquisition gradient-echo (MP-RAGE). Carotid artery morphology (wall volume, lumen volume, total vessel volume, normalized wall index, and mean/maximum wall thickness) and plaque component size (lipid rich/necrotic core, calcification, and hemorrhage) were measured over two time points.

Results: After exclusion of images with poor image quality, 257 matched locations from 18 subjects were available for analysis. For the quantitative carotid morphology measurements, coefficient of variation (CV) ranged from 2% to 15% and intraclass correlation coefficient (ICC) ranged from 0.87 to 0.99. Except for maximum wall thickness (ICC = 0.87), all ICC were larger than 0.90. For the quantitative plaque composition measurements, the ICC of the volume and relative content of lipid rich/necrotic core and calcification were larger than 0.90 with CV ranging from 22% to 32%.

Conclusion: The results from the multicontrast high-resolution 3T MR study show high reliability for carotid morphology and plaque component measurements. 3T MRI is a reliable tool for longitudinal clinical trials, with shorter scan time compared to 1.5T.

Key Words: carotid artery; atherosclerosis; magnetic resonance imaging; reproducibility; vessel wall
J. Magn. Reson. Imaging 2010;31:168–176.

HIGH-RESOLUTION MRI of carotid atherosclerotic plaque has recently gained a significant clinical interest as a tool capable of precise measurements of morphological features and tissue composition of atherosclerotic lesions (1–3). It has been established (4) that the presence of certain features, such as fibrous cap rupture, large lipid rich/necrotic core (LR/NC), and intraplaque hemorrhage (IPH) significantly increases the risk of cerebrovascular ischemic events (stroke and transient ischemic attacks). Beyond diagnostic and prognostic applications, carotid MRI has been widely used during recent years in clinical trials investigating the effect of lipid-lowering therapies (5,6). For such studies, MRI can deliver direct quantitative measures characterizing plaque size, geometry, and tissue composition, which are of critical interest as surrogate endpoints reflecting the effect of intervention on its primary target.

The use of MRI in therapeutical trials requires knowledge regarding the reproducibility of quantitative plaque measurements as key information for trial planning. Several studies reported interscan reproducibility of plaque morphological measurements and tissue composition using 1.5T scanners (7,8). The new generation of MRI scanners operating at a magnetic field of 3T has recently demonstrated a number of advantages for carotid plaque imaging due to an increased signal-to-noise ratio (SNR), improved spatial resolution, and a reduced scan time (9). While these benefits may promote a wider applications carotid MRI in clinical trials, it is unclear whether previous

[1]Department of Radiology, University of Washington, Seattle, Washington, USA.
[2]Department of Radiology, Peking University First Hospital, Beijing, China.
[3]Department of Surgery, University of Washington, Seattle, Washington, USA.
[4]Clinical Sites Research Program, Philips Research North America, New York, USA.
Contract grant sponsor: Pfizer, Groton, CN, USA.
*Address reprint requests to: C.Y., Vascular Imaging Lab, Department of Radiology, University of Washington, 815 Mercer Street, Seattle, WA 98109. E-mail: cyuan@u.washington.edu
Received May 22, 2009; Accepted October 5, 2009.
DOI 10.1002/jmri.22014
Published online in Wiley InterScience (www.interscience.wiley.com).

Table 1
Patient Population and Lesion-Type Distribution

	Mean ± SD or % (range or ratio)
A. Demography ($N = 20$)	
Age (years)	71.1 ± 9.3 (54–88)
Weight (kg)	78.3 ± 19.9 (54–127)
Male sex	90% (18/20)
B. Carotid stenosis by ultrasound ($N = 20$)	
16–49%	70.0% (14/20)
50–79%	30.0% (6/20)
C. Modified AHA lesion type by MRI ($N = 18$)	
III	22.2% (4/18)
IV–V	33.3% (6/18)
VI	22.2% (4/18)
VII	22.2% (4/18)

AHA = American Heart Association.

estimates of quantitative reproducibility based on 1.5T platforms (7,8) can be applied to 3T imaging, and whether the use of 3T scanners can improve precision of plaque measurements. Recently, two studies addressed scan-rescan reproducibility of carotid wall morphological measurements at 3T (10,11) based on relatively small populations of either healthy subjects (10) or patients with moderate disease and the absence of clinically significant stenosis (11). Therefore, it would be of further interest to evaluate the reproducibility in a larger population with clinically significant disease, which is the primary target for prospective therapeutic interventions.

Another aspect of plaque imaging reproducibility at 3T, which has not been addressed to date, is the measurements of plaque composition. Plaque segmentation based on multicontrast MRI allows quantitative determination of major plaque tissue components (LR/NC, calcification [CA], and hemorrhage) and their proportion to the fibrous matrix (3,12). These measurements are thought to provide valuable biomarkers for monitoring of therapy and disease progression. Particularly, the size and/or relative content of the LR/NC have been recently suggested as a primary endpoint for lipid-lowering interventions (5,13). The hemorrhage size has been shown to be an independent predictor of accelerated plaque progression (14,15). Reproducibility of plaque composition measurements at 1.5T was reported previously (8). However, carotid imaging at 1.5T poses a significant challenge due to SNR limitations and a long scan time. Multicontrast carotid imaging at 3T has been shown to allow considerable improvement in time efficiency (9), and, therefore, needs to be further evaluated in the context of measurement reproducibility for prospective serial clinical applications.

The purpose of this study was to evaluate interscan reproducibility of both plaque morphological and tissue composition measurements at 3T with the use of a fast optimized multicontrast protocol in the population with clinically significant carotid atherosclerosis.

MATERIALS AND METHODS

Subjects

A total of 20 patients (age range = 54–88; mean age = 71.05 ± 9.33 years; two females) with carotid stenosis >15% as identified by duplex ultrasound were recruited for two independent 3T MRI scans within one month. Details of patient population are given in Table 1.

The average interval of repeated scans was 12 days. No cardiovascular or cerebrovascular events were reported between the two scans. The arterial side with more severe stenosis, referred to as the index carotid artery, was selected for evaluation. Institutional

Table 2
Scan Parameters for the Carotid Imaging Protocol at 3T

	Scan type				
	1	2	3	4	5
Parameters	Black-blood PDW	Black-blood T2W	Black-blood T1W	Bright-blood TOF	MP-RAGE
Sequence	TSE	TSE	TSE	FFE	IR-TFE
Image mode	2D	2D	2D	3D	3D
Scan plane	Axial	Axial	Axial	Axial	Axial
TR (msec)	4000	4000	800	20	13
TE (msec)	8	50	10	4	4
FOV (cm)	14 × 14	14 × 14	14 × 14	14 × 14	14 × 14
Matrix size	256 × 256	256 × 256	256 × 256	256 × 256	256 × 256
Resolution (mm^2)	0.55 × 0.55	0.55 × 0.55	0.55 × 0.55	0.55 × 0.55	0.55 × 0.55
Slice thickness (mm)	2	2	2	1	1
Slices	16	16	16	32	32
Blood suppression	MDIR (TI = 230 msec)	MDIR (TI = 230 msec)	QIR (TI1/TI2 = 382/138 msec)	Saturation-veins	None
Special parameters	Echo train = 12; slices/TR = 8	Echo train = 12; slices/TR = 8	Echo train = 10	Flip angle = 20°	Flip angle = 15°; TI = 490 msec
Fat suppression	Yes	Yes	Yes	No	Yes
NEX	1	1	1	1	1
Scan time (minutes)	3	3	6	3	3

NEX = number of excitations, TSE = turbo spin-echo, FFE = fast field echo; IR = inversion-recovery, TFE = turbo field echo, MDIR = multislice double IR (16); QIR = quadruple IR (17).

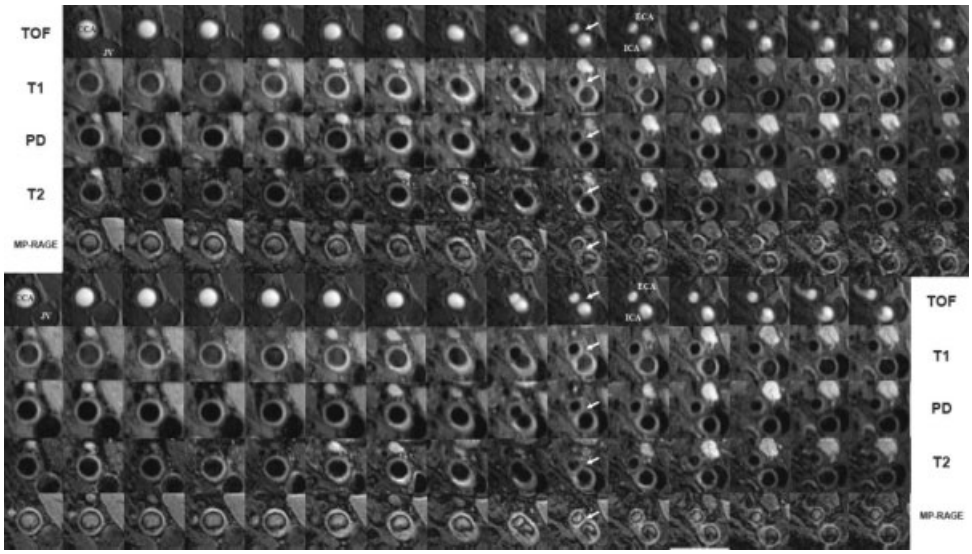

Figure 1. Example set of cross-sectional images with five contrast weightings obtained in two scanning sessions. Image registration relative to carotid bifurcation (arrow) results in 14 available locations (out of 16) for analysis, which were covered in both scanning sessions. From top to bottom: TOF, T1, PD, T2, and MP-RAGE at scan and rescan. Vessels are labeled as follows: CCA = common carotid artery, ICA = internal carotid artery, ECA = external carotid artery, JV = jugular vein.

review board approval was obtained and all subjects gave informed consent.

MRI Protocol

All MRI examinations were performed on a 3T (Achieva; Philips Medical Systems, Best, the Netherlands) platform using a bilateral four-element phased-array surface coil. A standardized protocol included five sequences applied in the transverse plane: 2D black-blood (BB) T1-weighted turbo spin-echo (TSE), 2D BB T2-weighted TSE, 2D proton-density-weighted BB TSE, 3D time-of-flight (TOF) MR angiography, and 3D magnetization-prepared rapid acquisition gradient-echo (MP-RAGE) (Table 2). Fat suppression was applied in all BB sequences and MP-RAGE to improve identification of vessel outer wall boundaries as well as to avoid chemical shift artifacts. Prior to the above sequences, the standard three-plane localization sequence was executed. Then, the two-step procedure was applied to localize the carotid bifurcation, as described elsewhere (18). This included fast 2D TOF MR angiography in the transverse plane and oblique 2D BB TSE sequence with scan times of 2 and 1.5 minutes, respectively. To ensure registration between two scanning sessions, images were centered at the carotid bifurcation of the index artery, which was defined as the most stenotic artery based on prior ultrasound screening. The longitudinal coverage was 32 mm, extending from the common carotid artery to internal carotid artery. After acquisition, all raw data were interpolated to a matrix size of 512 × 512 pixels. The total scan time including localization sequences and image planning was less than 25 minutes.

Image Analysis

Before image review, cross-sectional images of five weightings from each index artery were matched by one radiologist (H.U.) using the bifurcation of common carotid artery as a fiducial marker (Fig. 1). Two reviewers (F.L. and H.Z.) with at least one year experience in carotid MRI imaging reviewed the images. Both reviewers were blinded to the scan session and subject. Image sets of each subject obtained during the first and second scanning session were randomized and interpreted separately to avoid any potential bias in repeated readings of the same subject. Each axial location was read by two reviewers who reached consensus decision. Image quality (IQ) was assessed using a four-point scale on which a score of 1 indicated poor quality and 4 indicated excellent (19). Imaging locations with an average image quality <2 were excluded from study. A custom-designed image analysis software (CASCADE) (20) was used to outline the lumen area (LA) and total vessel area (TVA) as well as plaque components. Wall area (WA = TVA – LA), normalized wall index (NWI = WA/TVA), mean wall thickness (MWT), and maximal wall thickness (MaxWT) measures were derived from the LA and TVA outlines. Wall volume (WV), lumen volume (LV), and total vessel volume (TVV) were obtained by summing area measurements for each artery and multiplying by slice thickness (2 mm). Criteria for delineating IPH, LR/NC, and CA were based on previous publications (3,21). Absolute volumes of plaque components and their percentage (%) in the WV were recorded. For error analysis across artery segments, the carotid artery was divided into three parts: 1) common, >4 mm proximal to the bifurcation; 2) carotid bulb, 0 to 4 mm proximal to the bifurcation; and 3) internal, >0 mm distal to the bifurcation (22). In addition, each lesion was classified on the artery basis according to modified American Heart Association (AHA) criteria (type I–VII) (1).

Statistical Analysis

A paired *t*-test was performed to compare the quantitative measurement between two scan sessions. Measurement error (coefficient of variation [CV]) was calculated as 100% × $\sqrt{}$[within-patient variance]/mean

Table 3
Interscan Reproducibility Results for Carotid Morphology Volume Measurement

Parameter	Scan (mean ± SD)	Rescan (mean ± SD)	*P* value[a]	CV (%)	ICC (95% CI)
Lumen volume (mm^3)	1097.21 ± 335.68	1083.11 ± 336.56	0.14	2.60	0.99 (0.98–1.00)
Wall volume (mm^3)	743.73 ± 122.43	733.19 ± 126.43	0.32	4.20	0.94 (0.84–0.98)
Total vessel volume (mm^3)	1840.94 ± 358.70	1816.30 ± 354.48	0.07	2.25	0.99 (0.97–1.00)
Mean wall thickness (mm)	1.08 ± 0.26	1.08 ± 0.27	0.90	3.87	0.97 (0.93–0.99)
Max wall thickness (mm)	3.12 ± 1.30	3.19 ± 1.35	0.63	14.79	0.87 (0.69–0.95)
Normalized wall index[b]	0.41 ± 0.08	0.41 ± 0.09	0.98	3.02	0.98 (0.94–0.99)

[a]Paired *t*-test for interscan measurements.
[b]Wall volume/total vessel volume.
CV = coefficient of variation, ICC = intraclass correlation coefficient, CI = confidence interval.

(all measurements) (8). Intraclass correlation coefficient (ICC) was calculated to evaluate the agreement between repeated measurements. An ICC of less than 0.40 is considered poor agreement, one between 0.40 and 0.75 is considered fair, and one greater than 0.75 is considered excellent (23). The mean differences between repeated scans against the mean value of repeated scans were described by Bland-Altman plots. The bias was examined using the paired *t*-test. The agreement of detection of plaque components was assessed with Cohen's kappa (slight agreement = 0.00–0.20; fair = 0.21–0.40; moderate = 0.41–0.60; substantial = 0.61–0.80; near-perfect = 0.81–1.00) (24). Statistical significance was defined at $P < 0.05$. All analyses were performed in SPSS for Windows (version 12.0; Chicago, IL, USA).

RESULTS

All 20 patients recruited in this study completed both scan sessions. Two patients were excluded from analysis due to poor image quality. After image registration and exclusion of three locations with image quality less than 2, 257 matched locations from 18 subjects were available for analysis. Note that 28 of 288 locations corresponding to the remaining subjects were unavailable for analysis due to misregistration despite acceptable image quality. Lesion distribution in the studied population (Table 1) appeared rather uniform across lesion types according to modified AHA criteria.

Reproducibility of Quantitative Carotid Morphology Measurements

Results for interscan reproducibility of carotid morphology measurement are provided in Table 3. No significant difference was found between repeated scans ($P > 0.05$). CV ranged from 2.25% to 14.79%. Measurement error for the location-based measurements (maximum wall thickness) was considerably larger than those of artery-based measurements (volumes and mean wall thickness). Interscan agreement for quantitative morphology measurements was excellent, with ICC ranging from 0.87 to 0.99. Except for maximum wall thickness (ICC = 0.87), all ICC were greater than 0.90. Bland-Altman plots for interscan measurements (Fig. 2a–f) demonstrate random error scattering patterns with no significant bias and no significant correlation between bias and mean. Analysis of measurement precision for three artery segments is presented in Table 4. Compared to other artery segments, the carotid bulb showed lower ICC and larger errors for all morphological measurements (Table 4).

Reproducibility of Quantitative Carotid Plaque Composition Measurements

Among 18 subjects, 11 presented plaques containing LR/NC, 13 presented calcifications, and in two cases IPH was detected. All calcifications and hemorrhages were repeatedly detected on both scans in the same subjects (perfect agreement with kappa = 1). Out of 11 subjects presenting LR/NC on at least one scan, in two subjects it was detected on one scan only, resulting in kappa = 0.78. For further reproducibility analysis, the undetected LR/NC on corresponding scans in these two subjects were assigned with zero volumes. No statistical analysis was performed for quantitative measurements of IPH due to the small number of positive cases.

Statistical analysis for reproducibility of plaque tissue composition is presented in Table 5. The ICC values indicated excellent agreements for the measurements of volume and relative content of all components with ICC > 0.9. CV ranged from 21.90% to 31.74%. Bland-Altman plots for scan-rescan volume measurements of LR/NC and calcified tissue (Fig. 2g and h) demonstrate the absence of any significant bias and no significant correlation between bias and mean. Examples of the appearance of major plaque components on repeated scans are presented in Figs. 3–5 for LR/NC, CA, and hemorrhage, respectively.

DISCUSSION

This study provides the first comprehensive assessment of scan-rescan variations of both gross morphological measurements of the atherosclerotic plaque and its tissue composition using MRI at 3T. It is also important to emphasize that the patient population in our study is considerably larger than those in previous 3T reproducibility studies (10,11). In general, our data indicate excellent reproducibility for all measurements obtained from carotid images with acceptable image quality. The reproducibility was slightly lower for the location-specific parameter (MaxWT) than for measurements based on the whole artery volume (all ICC > 0.9). Thus, volume-based measurements would

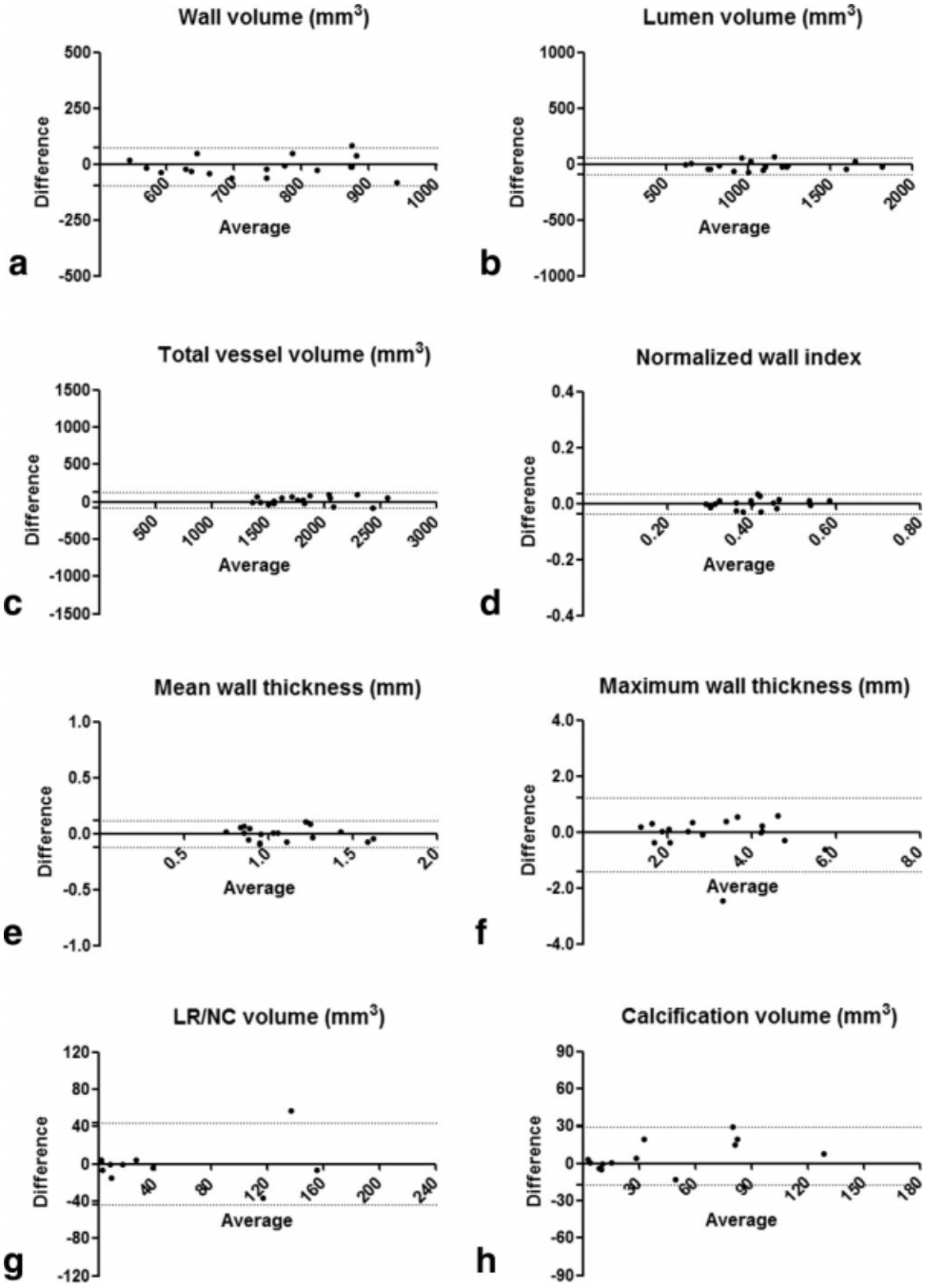

Figure 2. Bland-Altman plots for the carotid artery morphology and plaque component volume measurements. No significant bias was found for all parameters ($P > 0.05$). The dashed lines indicate 95% limits of agreement.

be preferable for clinical studies due to better reliability.

Compared to previous studies based on 1.5T (7,8) and 3T (10,11) MRI, our estimates of scan-rescan reproducibility of plaque morphological parameters appear to be very similar. Particularly, both ICC and CV found in this study for gross morphological measurements (LV, WV, TVV, and NWI) are in good agreement with earlier publications based on either single-contrast measurements (10,11) or a multicontrast protocol (8). Overall, our and previous work confirms a high reliability of plaque morphology measurements, though no improvement was found at 3T compared to 1.5T (7–10). Furthermore, this conclusion is in agreement with the recent study by Vidal et al (11), which demonstrated no improvement of reproducibility in direct comparison between 1.5T and 3T platforms, despite a significant increase in SNR at 3T. These findings suggest that optimally designed protocols for both field strengths currently provide the highest available precision of plaque morphology measurements in a clinical setting.

The residual variability is unlikely to be related to instrumental factors and rather caused by patient positioning variations and corresponding image misregistration. It should be pointed out that both this and previous studies (8,11) utilized the protocols with highly nonisotropic spatial resolution, where the slice thickness (typically 2 mm) is much larger than the in-plane resolution (pixel size is typically 0.4–0.6 mm). These resolution parameters are commonly used in

Table 4
Interscan Reproducibility Results for Morphology Measurement Based on Artery Segments

Segment	Scan (mean ± SD)	Rescan (mean ± SD)	*P* value[a]	CV (%)	ICC (95% CI)
CCA					
Lumen volume (mm^3)	374.08 ± 127.55	364.92 ± 126.43	0.06	3.80	0.99 (0.97–1.00)
Wall volume (mm^3)	183.39 ± 54.85	181.30 ± 59.21	0.58	5.80	0.96 (0.90–0.99)
Total vessel volume (mm^3)	557.47 ± 162.01	546.22 ± 161.41	0.11	3.72	0.99 (0.96–1.00)
Mean wall thickness (mm)	0.86 ± 0.19	0.86 ± 0.21	0.94	4.95	0.95 (0.88–0.98)
Normalized wall index[b]	0.33 ± 0.07	0.33 ± 0.07	0.70	3.63	0.97 (0.92–0.99)
Carotid bulb					
Lumen volume (mm^3)	329.41 ± 131.67	332.41 ± 143.75	0.69	6.48	0.98 (0.93–0.99)
Wall volume (mm^3)	220.19 ± 57.17	216.68 ± 55.43	0.60	8.95	0.87 (0.70–0.95)
Total vessel volume (mm^3)	549.60 ± 142.80	549/08 ± 145.75	0.96	5.55	0.95 (0.88–0.98)
Mean wall thickness (mm)	1.21 ± 0.33	1.21 ± 0.37	0.89	8.09	0.92 (0.80–0.97)
Normalized wall index[b]	0.41 ± 0.10	0.41 ± 0.11	0.76	6.14	0.95 (0.86–0.98)
ICA					
Lumen volume (mm^3)	414.51 ± 202.47	406.06 ± 200.58	0.20	4.71	0.99 (0.98–1.00)
Wall volume (mm^3)	350.34 ± 92.55	345.29 ± 74.50	0.46	5.66	0.94 (0.86–0.98)
Total vessel volume (mm^3)	764.85 ± 226.40	751.34 ± 212.91	0.10	3.21	0.99 (0.97–1.00)
Mean wall thickness (mm)	1.15 ± 0.42	1.16 ± 0.42	0.77	6.78	0.96 (0.90–0.99)
Normalized wall index[b]	0.48 ± 0.15	0.49 ± 0.15	0.55	4.02	0.98 (0.96–0.99)

[a]Paired *t*-test for interscan measurements.
[b]Wall volume/total vessel volume.
CCA = common carotid artery, ICA = internal carotid artery, CV = coefficient of variation, ICC = intraclass correlation coefficient, CI = confidence interval.

modern carotid MRI as a tradeoff between several technical challenges, such as a low SNR, long scan time, and blood suppression efficiency related to the slice thickness in double inversion-recovery (DIR) techniques (25,26). It has recently been demonstrated (18) that highly nonisotropic spatial resolution (i.e., a large slice thickness) is a major source of error in plaque morphological measurements due to variations of patients' positioning between repeated scans. Our analysis of measurement variability across artery segments (Table 4) further supports this conclusion. Although for each segment of the carotid artery, interscan agreements were excellent with ICC > 0.8, the reproducibility was not consistent between different segments. Specifically, the carotid bulb showed the lowest ICC and the largest CV in the measurements of WV, LV, TVV, MWT, and NWI. This finding can be easily explained in view of errors caused by nonisotropic resolution, as the bifurcation region is characterized by high anatomical variability. Correspondingly, a variety of angulations between the vessel wall and imaging plane can occur during slice positioning across subjects and repeated scans. On the other hand, relatively straight segments of the common and internal carotid arteries facilitate easier setting of orthogonal cross-sectional geometry, which is preferable for contour-based measurements. While this limitation is unavoidable within current protocol designs based on 2D sequences, further improvements in measurement precision and accuracy would likely require application of 3D sequences with isotropic or nearly-isotropic spatial resolution (26) and more sophisticated 3D registration postprocessing techniques. However, a long scan time and associated problems with patient motion remain the major limitation of 3D BB imaging to date (26).

An important aspect of this study is that it was performed on a typical clinical population of subjects presenting a wide range of disease severity, as indicated by % stenosis and lesion type distribution (Table 1). Correspondingly, imaging data allowed estimating the reproducibility of plaque component measurements for LR/NC and calcified tissue. Detection and quantitative measurements of LR/NC and CA provided generally very good agreement, with ICC > 0.9, similar to previous data at 1.5T (8). Compared to the literature (8), our measurements for calcified tissue showed a slightly reduced variability (CV = 22% in this study vs. 31% in Ref. 8). This finding is in accord with the recent report by Underhill et al (19), which demonstrated an apparent increase of calcification prevalence and size at 3T compared to 1.5T and attributed this effect to an increase of magnetic

Table 5
Interscan Reproducibility for Plaque Composition Volume Measurement

Component	Scan (mean ± SD)	Rescan (mean ± SD)	*P* value[a]	CV (%)	ICC (95% CI)
LR/NC (mm^3)[b]	47.22 ± 58.21	47.25 ± 62.31	0.99	31.74	0.93 (0.77–0.98)
Calcification (mm^3)[b]	38.16 ± 37.22	44.05 ± 43.51	0.10	21.96	0.96 (0.87–0.99)
% LR/NC (%)[b]	6.20 ± 7.34	6.18 ± 7.56	0.98	24.76	0.95 (0.84–0.99)
% Calcification (%)[b]	4.63 ± 4.06	5.43 ± 4.88	0.06	21.90	0.95 (0.85–0.99)

[a]Paired *t*-test for interscan measurements.
[b]Only arteries that exhibited the feature in at least one time point were included; $N = 11$ for LR/NC, $N = 13$ for calcification.
LR/NC = lipid-rich/necrotic core, CV = coefficients of variation, ICC = intraclass correlation coefficient, CI = confidence interval.

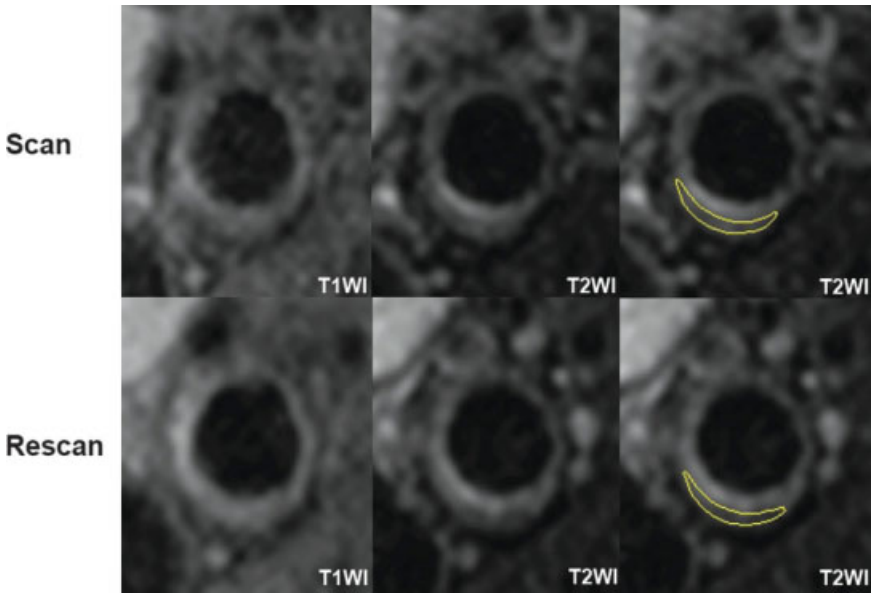

Figure 3. The typical image pattern of lipid rich/necrotic core (LR/NC) is isointensity on T1-weighted imaging (T1WI) and low intensity on T2-weighted imaging (T2WI). In the posterior vessel wall, a crescent LR/NC could be found with a good agreement of size and shape between two scans. LR/NC = yellow.

susceptibility in a higher field. On the contrary, LR/NC measurements demonstrated a reduced precision relative to 1.5T data (ICC = 0.93 vs. 0.99 [Ref. 8] and CV = 32% vs. 11% [Ref. 8]). While there is no unambiguous interpretation of this observation, several possible reasons need to be mentioned. First, the difference in within-subject variations can be addressed to the population distinctions alone. Particularly, Saam et al (8) reported a considerably larger population-average LR/NC volume (140 mm^3) and relative content (14%) compared to our study (47 mm^3 and 6%, respectively, as shown in Table 5). Therefore, the difference in CV can be related to the absolute size of LR/NC, as smaller regions tend to produce larger relative errors. Second, a reduced precision can be caused by the absence of contrast-enhanced (CE) T1-weighted imaging in our protocol. Cai et al (27) demonstrated that CE MRI has a superior capability of LR/NC visualization compared to T2-weighted imaging. Literature data (8) are based on CE measurements, and therefore may be more accurate. Third, the distinctions also can be attributed to the image review methodology. While this work is based on the completely blinded image analysis procedure, in the study by Saam et al (8) image review for all repeated scans was performed simultaneously. Such an analysis technique is prone to an artificial reduction of variability, as an operator tends to introduce more similarity in contours outlining a region-of-interest visible on a series of scans compared to the situation when only a single scan is available for review. Finally, it should be noted that current literature about statistical aspects of quantitative characterization of plaque composition is very limited (8), and further research is needed to identify optimal protocols and image analysis techniques for LR/NC measurements.

While scan-rescan reproducibility of plaque measurements at 3T found in this study was essentially similar to 1.5T (7,8), the use of a higher field strength offers a clear advantage of reducing the scan time. This scan-time reduction is a direct consequence of an increased SNR, which allows using a single signal average for all imaging sequences instead of two averages typically used at 1.5T (9). The fast carotid MRI protocol implemented in this work affords a comprehensive multicontrast examination in less than 25 minutes, thus providing a capability of routine clinical applications in large-scale studies. Compared to previously published 1.5T protocols (5), our protocol allows for an about 40% to 50% reduction of the scan time. Correspondingly, 3T carotid MRI offers a promise of becoming a routine screening tool for both epidemiological surveys and practical healthcare.

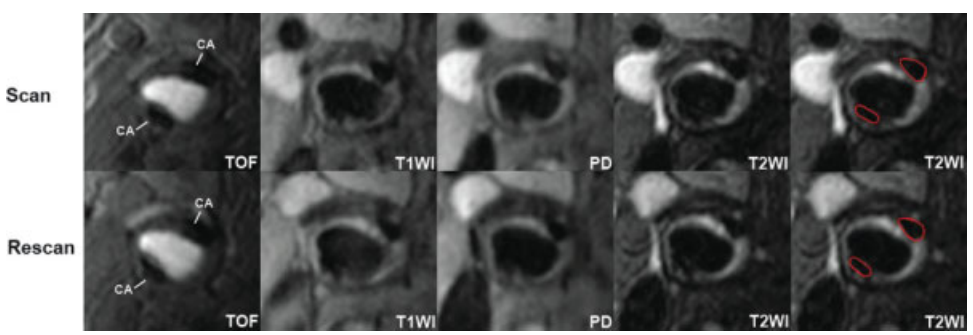

Figure 4. Calcification (CA) shows dark signal on TOP, T1-weighted imaging (T1WI), PD, and T2-weighted imaging (T2WI). At the same location of repeated scans, calcification could be detected with high reliability. Calcification = red.

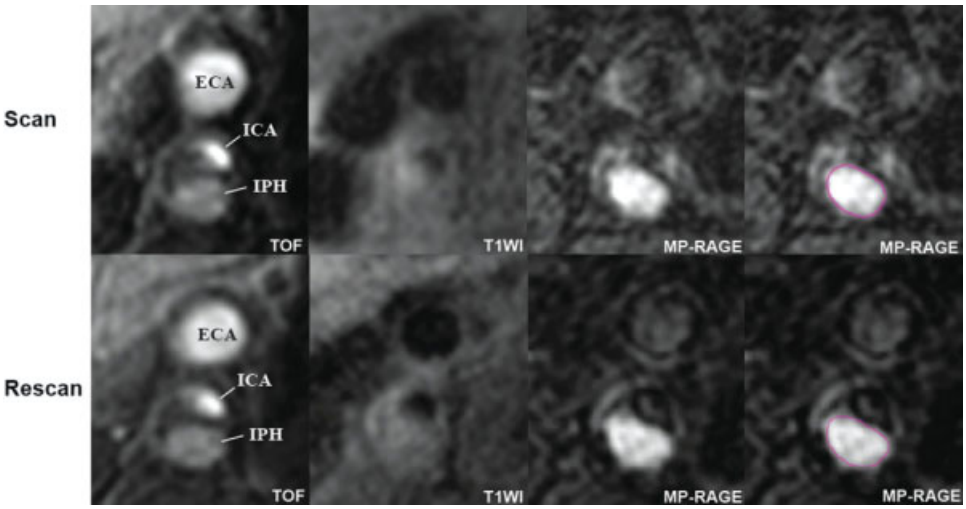

Figure 5. The intraplaque hemorrhage (IPH) area showed much higher signal intensity and clearer boundary on MP-RAGE, compared with TOF and T1-weighted imaging (T1WI). With this character, MP-RAGE can identify IPH more reliable at repeated scans. ECA = external carotid artery, ICA = internal carotid artery; hemorrhage = pink. [Color figure can be viewed in the online issue, which is available at www.interscience.wiley.com.]

Two limitations of this study need to be pointed out. First, as noted above, we did not use a CE imaging protocol, which potentially could reduce errors of LR/NC measurements. It is reasonable to believe that CE MRI can be beneficial for longitudinal clinical trials focused on the observation of LR/NC changes (27). On the other hand, gadolinium contrast agents were linked to an increased risk of nephrogenic systemic fibrosis (NSF) (28). Current practice of contrast administration requires additional screening for impaired kidney function, which may reduce an available patient population. In view of this circumstance, future carotid MRI clinical studies will likely employ a dual strategy: either noncontrast cost-efficient screening in large populations or precise LR/NC size monitoring using CE in smaller prescreened populations with the absence of clinical contradictions and a detectable LR/NC. In this aspect, our data can be used for planning of population-based noncontrast studies, while the reproducibility of contrast-based LR/NC measurements at 3T remains a topic for future research. Second, the sample size and population structure of this study was insufficient for quantitative analysis of IPH, as only two cases were identified. Given the clinical importance of IPH (14,29), a future study needs to be designed to quantitatively investigate this aspect of plaque composition based on a prescreened population with advanced lesions. It also should be pointed out that our data (Fig. 5) qualitatively support recent findings (21,30) regarding an advantage of the MP-RAGE sequence compared to T1-weighted TSE and TOF for detection of IPH at 3T.

In conclusion, the results from this multicontrast high-resolution 3T MRI study show high reproducibility for carotid plaque morphology and tissue composition measurements, comparable to previously reported 1.5T and 3T data. These results prove that MRI is a reliable tool for clinical studies focused on the natural history and therapy of atherosclerosis. The main advantage of 3T imaging for such studies is the improvement in time efficiency, which enables fast screening examinations in a clinical setting.

REFERENCES

1. Cai JM, Hatsukami TS, Ferguson MS, Small R, Polissar NL, Yuan C. Classification of human carotid atherosclerotic lesions with in vivo multicontrast magnetic resonance imaging. Circulation 2002;106:1368–1373.
2. Fabiano S, Mancino S, Stefanini M, et al. High-resolution multicontrast-weighted MR imaging from human carotid endarterectomy specimens to assess carotid plaque components. Eur Radiol 2008;18:2912–2921.
3. Saam T, Ferguson MS, Yarnykh VL, et al. Quantitative evaluation of carotid plaque composition by in vivo MRI. Arterioscler Thromb Vasc Biol 2005;25:234–239.
4. Takaya N, Yuan C, Chu B, et al. Association between carotid plaque characteristics and subsequent ischemic cerebrovascular events: a prospective assessment with MRI-initial results. Stroke 2006;37:818–823.
5. Underhill HR, Yuan C, Zhao XQ, et al. Effect of rosuvastatin therapy on carotid plaque morphology and composition in moderately hypercholesterolemic patients: a high-resolution magnetic resonance imaging trial. Am Heart J 2008;155:584.e1–584.e8.
6. Corti R, Fuster V, Fayad ZA, et al. Effects of aggressive versus conventional lipid-lowering therapy by simvastatin on human atherosclerotic lesions: a prospective, randomized, double-blind trial with high-resolution magnetic resonance imaging. J Am Coll Cardiol 2005;46:106–112.
7. Kang X, Polissar NL, Han C, Lin E, Yuan C. Analysis of the measurement precision of arterial lumen and wall areas using high-resolution MRI. Magn Reson Med 2000;44:968–972.
8. Saam T, Kerwin WS, Chu B, et al. Sample size calculation for clinical trials using magnetic resonance imaging for the quantitative assessment of carotid atherosclerosis. J Cardiovasc Magn Reson 2005;7:799–808.
9. Yarnykh VL, Terashima M, Hayes CE, et al. Multi-contrast black-blood MRI of carotid arteries: comparison between 1.5 and 3 Tesla magnetic field strengths. J Magn Reson Imaging 2006;23:691–698.
10. Alizadeh Dehnavi R, Doornbos J, Tamsma JT, et al. Assessment of the carotid artery by MRI at 3T: a study on reproducibility. J Magn Reson Imaging 2007;25:1035–1043.
11. Vidal A, Bureau Y, Wade T, et al. Scan-rescan and intra-observer variability of magnetic resonance imaging of carotid atherosclerosis at 1.5 T and 3.0 T. Phys Med Biol 2008;53:6821–6835.
12. Clarke SE, Hammond RR, Mitchell JR, Rutt BK. Quantitative assessment of carotid plaque composition using multicontrast MRI and registered histology. Magn Reson Med 2003;50:1199–1208.
13. Zhao XQ, Yuan C, Hatsukami TS, et al. Effects of prolonged intensive lipid-lowering therapy on the characteristics of carotid atherosclerotic plaques in vivo by MRI: a case-control study. Arterioscler Thromb Vasc Biol 2001;21:1623–1629.

14. Kolodgie FD, Gold HK, Burke AP, et al. Intraplaque hemorrhage and progression of coronary atheroma. N Engl J Med 2003;349: 2316–2325.
15. Takaya N, Yuan C, Chu B, et al. Presence of intraplaque hemorrhage stimulates progression of carotid atherosclerotic plaques: a high-resolution magnetic resonance imaging study. Circulation 2005;111:2768–2775.
16. Yarnykh VL, Yuan C. Multislice double inversion-recovery black-blood imaging with simultaneous slice reinversion. J Magn Reson Imaging 2003;17:478–483.
17. Yarnykh VL, Yuan C. T1-insensitive flow suppression using quadruple inversion-recovery. Magn Reson Med 2002;48: 899–905.
18. Balu N, Kerwin WS, Chu B, Liu F, Yuan C. Serial MRI of carotid plaque burden: influence of subject repositioning on measurement precision. Magn Reson Med 2007;57:592–599.
19. Underhill HR, Yarnykh VL, Hatsukami TS, et al. Carotid plaque morphology and composition: initial comparison between 1.5- and 3.0-T magnetic field strengths. Radiology 2008;248:550–560.
20. Kerwin W, Xu D, Liu F, et al. Magnetic resonance imaging of carotid atherosclerosis: plaque analysis. Top Magn Reson Imaging 2007;18:371–378.
21. Zhu DC, Ferguson MS, DeMarco JK. An optimized 3D inversion recovery prepared fast spoiled gradient recalled sequence for carotid plaque hemorrhage imaging at 3.0T. Magn Reson Imaging 2008;26:1360–1366.
22. Saam T, Underhill HR, Chu B, et al. Prevalence of American Heart Association type VI carotid atherosclerotic lesions identified by magnetic resonance imaging for different levels of stenosis as measured by duplex ultrasound. J Am Coll Cardiol 2008;51: 1014–1021.
23. Fleiss JL. Reliability of measurement. In: Fleiss JL, editor. The design and analysis of clinical experiments, 1986 edition. New York: John Wiley and Sons Inc; 1986. p 1–31.
24. Landis JR, Koch GG. The measurement of observer agreement for categorical data. Biometrics 1977;33:159–174.
25. Edelman RR, Chien D, Kim D. Fast selective black blood MR imaging. Radiology 1991;181:655–660.
26. Balu N, Chu B, Hatsukami TS, Yuan C, Yarnykh VL. Comparison between 2D and 3D high-resolution black-blood techniques for carotid artery wall imaging in clinically significant atherosclerosis. J Magn Reson Imaging 2008;27:918–924.
27. Cai J, Hatsukami TS, Ferguson MS, et al. In vivo quantitative measurement of intact fibrous cap and lipid-rich necrotic core size in atherosclerotic carotid plaque: comparison of high-resolution, contrast-enhanced magnetic resonance imaging and histology. Circulation 2005;112:3437–3444.
28. Wiginton CD, Kelly B, Oto A, et al. Gadolinium-based contrast exposure, nephrogenic systemic fibrosis, and gadolinium detection in tissue. AJR Am J Roentgenol 2008;190:1060–1068.
29. Lusby RJ, Ferrell LD, Ehrenfeld WK, Stoney RJ, Wylie EJ. Carotid plaque hemorrhage. Its role in production of cerebral ischemia. Arch Surg 1982;117:1479–1488.
30. Ota H, Yarnykh VL, Ferguson MS, et al. Comparison between three T1-weighted sequences for detection and area measurement of intraplaque hemorrhage in carotid atherosclerotic plaque imaging at 3 Tesla. In: Proceedings of the 17th Annual Meeting of ISMRM, Honolulu, HI, USA, 2009 (Abstract 605).